

# Crustal deformation at the oblique spreading Reykjanes Peninsula, SW Iceland: GPS measurements from 1993 to 1998

Sigrún Hreinsdóttir<sup>1</sup> and Páll Einarsson

Science Institute, University of Iceland, Reykjavík, Iceland

Freysteinn Sigmundsson

Nordic Volcanological Institute, University of Iceland, Reykjavík, Iceland

**Abstract.** In 1993 and 1998 a 38-point GPS network was surveyed on the Reykjanes Peninsula, SW Iceland. According to the NUVEL-1A plate motion model the spreading rate of the North American and Eurasian plates in SW Iceland is  $18.9 \pm 0.5$  mm/yr toward  $N102.7^\circ \pm 1.1^\circ E$ , highly oblique to the plate boundary. Instead of oblique spreading, the measurements indicate left-lateral shear strain accumulation parallel to the Reykjanes Peninsula seismic zone ( $\sim N76^\circ E$ ) at the rate of about  $\dot{\epsilon}_{yx} \approx -0.2$   $\mu$ strain/yr (tensor shear strain). Subsidence is generally observed toward the seismic zone. A local maximum subsidence of 60 mm was measured in the Svartsengi geothermal area. Subsidence in this area has previously been detected with geodetic measurements and is considered a result of geothermal usage. Expansion was observed in the area of the Hengill triple junction. This is probably a result of magma accumulation beneath! mount Hrómundartindur, as previous seismic and geodetic measurements have indicated. Using a simple screw dislocation model, we fit the majority of the data. Assuming a left-lateral shear zone at depth along the seismic zone, we estimate locking depth of  $\sim 6.5$  km and deep slip rate of  $\sim 16.5$  mm/yr. The maximum left-lateral displacement predicted by the screw dislocation model,  $11.85 \pm 0.06$  mm/yr, is consistent with the observed value of  $11.9 \pm 0.5$  mm/yr. If the Hengill area is excluded, little extension is observed across the peninsula. The discrepancy between the NUVEL-1A oblique spreading and the observed transcurrent motion is thought to be caused by lack of magma intrusion into the crust during this time period.

## 1. Introduction

One of the effects of the Iceland mantle plume on the mid-Atlantic plate boundary is to break it up into a series of transform zones and rift zones, some of which are highly oblique. The Reykjanes Peninsula oblique rift in SW Iceland is one of these. It connects the Reykjanes Ridge offshore to other plate boundary segments in Iceland (Figure 1). In this area the relative plate velocity between the Eurasian and North American plates is  $18.9 \pm 0.5$  mm/yr toward  $N102.7^\circ \pm 1.1^\circ E$ , calculated from the NUVEL-1A plate motion model [DeMets *et al.*, 1990, 1994]. The Reykjanes Peninsula

plate boundary has a trend of  $\sim N76^\circ E$  (Figure 2). This highly oblique rift became active after a ridge jump from the Snæfellsnes rift, Snæfellsnes Peninsula (Figure 1),  $\sim 6$ -7 Ma ago [Sæmundsson, 1978; Jóhannesson, 1980; Kristjánsson and Jónsson, 1998]. The rift on the peninsula is marked by active, NE trending volcanic systems or spreading segments that are arranged en echelon along the zone. Each of the volcanic systems is associated with a high-temperature geothermal area. The rift structures of individual systems are oblique to the regional spreading direction as derived from the NUVEL-1A model and the obliqueness is in the same sense as that of the zone itself. Toward the east the plate boundary branches into the South Iceland Seismic Zone (SISZ) and the Western Volcanic Zone (WVZ) (Figure 1).

A large part of the Reykjanes Peninsula is covered by postglacial lavas [Sæmundsson and Einarsson, 1980], and all the volcanic systems have produced lavas in historic times, i.e., the last 1100 years. It has been suggested that volcanic activity on the peninsula is episodic. Periods of high volcanic activity, lasting a few

<sup>1</sup>Now at Geophysical Institute, University of Alaska Fairbanks, Fairbanks, Alaska.

Copyright 2001 by the American Geophysical Union.

Paper number 2001JB000428.

0148-0227/01/2001JB000428\$09.00

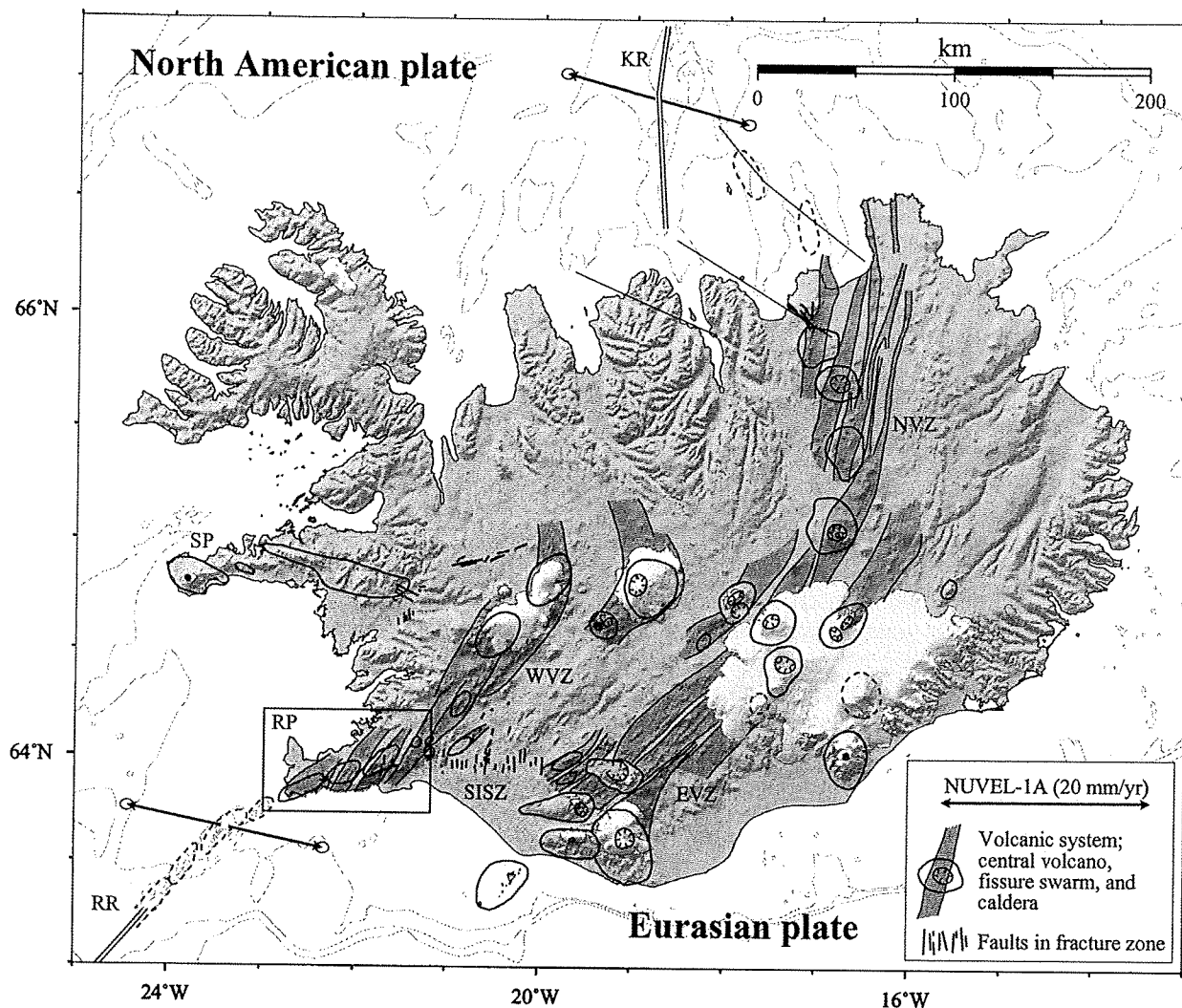


**Figure 1.** Iceland. The onland plate boundary between the North American and Eurasian plate is marked by volcanic systems and fracture zones. The arrows indicate the NUVEL-1A spreading rate, and the box shows the study area, Reykjanes Peninsula. Location's of fractures and volcanic systems are from *Einarsson and Sæmundsson* [1987] and *Árnason et al.* [1986]; location of faults in the SISZ are from *Einarsson* [1996], and location's of faults on the Reykjanes Peninsula are from P. Einarsson et al. (manuscript in preparation, 2001). RR, Reykjanes Ridge; RP, Reykjanes Peninsula; SP, Snæfellsnes Peninsula; SISZ, South Icelandic Seismic Zone; WVZ, Western Volcanic Zone; EVZ, Eastern Volcanic Zone; NVZ, Northern Volcanic Zone; KR, Kolbeinsey Ridge.

hundred years, are followed by volcanically quiet periods that last several hundred years. Each cycle thus lasts of the order of 1000 years [Sigurgeirsson, 1992]. The last major magmatic episode on the peninsula occurred in the tenth to the thirteenth century, and the last known eruption on Reykjanes Peninsula occurred around 1240 A.D. [Jóhannesson and Einarsson, 1998].

In volcanically quiet periods the Reykjanes Peninsula appears to be seismically very active. Earthquakes and earthquake swarms have been frequent on the peninsula in the last century, with the largest events exceeding magnitude 6 [Erlendsson, 1996]. However, excluding the Hengill area, the peninsula has been relatively quiet from 1974 to 1999, following a period of high activity in 1967-1973 [Einarsson, 1991].

Seismic studies suggest that the seismicity follows a narrow zone along the peninsula rather than the fissure swarms (Figure 2). The seismic zone lies along the whole peninsula with the average trend of  $\sim 80^\circ\text{E}$  [Einarsson, 1991]. About 90% of the detected earthquakes occur at depths of  $\sim 1\text{-}5$  km with the focal mechanism of normal faulting or strike-slip movement [Klein et al., 1973, 1977; A. Tryggvason et al., Three-dimensional imaging of the *P*- and *S*-wave velocity structure and earthquake locations beneath southwest Iceland, submitted to , 2000 (hereinafter cited as A. Tryggvason et al., submitted manuscript, 2000)]. In or near this narrow seismic zone, ground observations have shown N-S trending, right-lateral strike slip faults, indicating bookshelf style of deformation (left lateral)

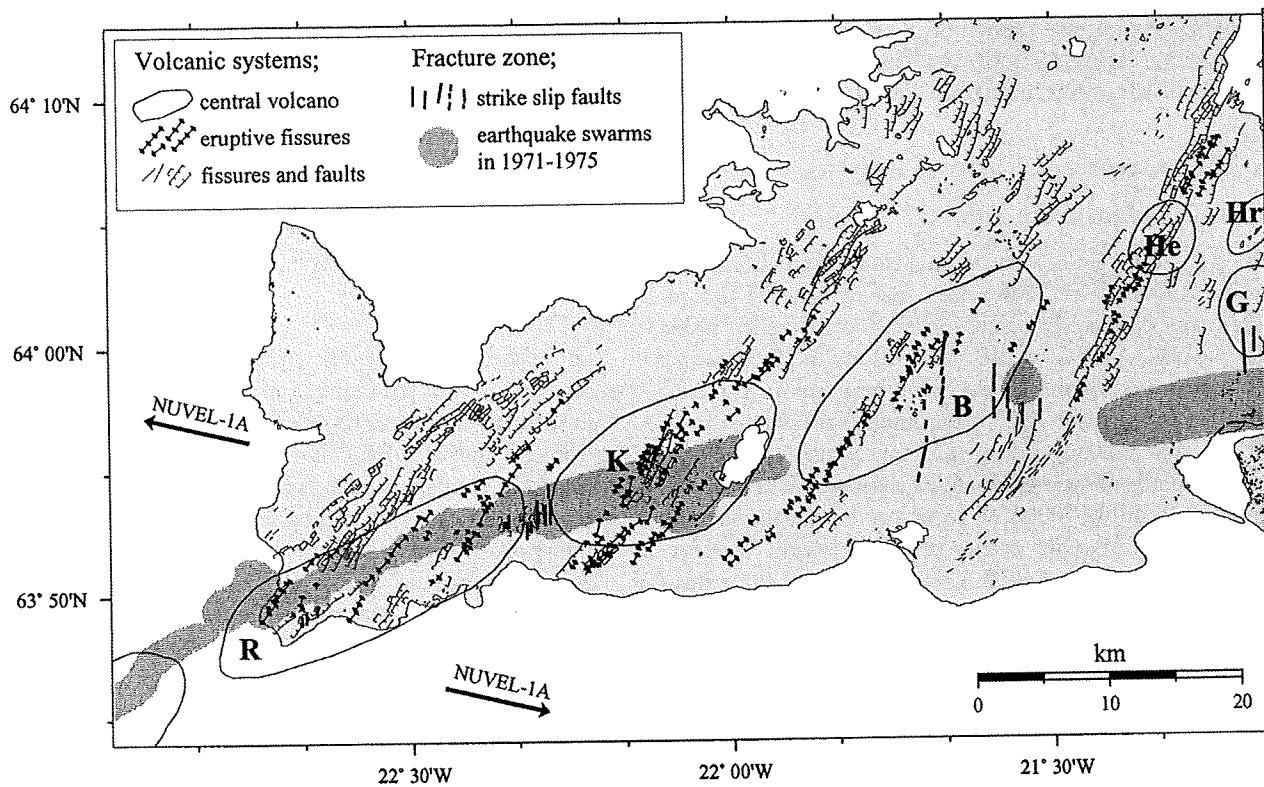


**Figure 2.** Volcanic systems and fracture zone on the Reykjanes Peninsula. The shaded area shows location of earthquake swarms in 1971-1975 [Einarsson and Björnsson, 1992], and letters indicate volcanic systems: R, Reykjanes; K, Krísuvík; B, Brennisteinsfjöll; He, Hengill; Hr, Hrómundartindur; G, Grensdalur. Central volcanos are from Árnason et al. [1986] and Einarsson and Sæmundsson [1987], fissures and faults are from Sæmundsson and Einarsson [1980], and N-S trending strike-slip faults are from P. Einarsson et al. (manuscript in preparation, 2001).

along the E-W trending seismic zone (P. Einarsson et al., manuscript in preparation, 2001).

Leveling and tilt measurements have been performed on numerous profiles on the Reykjanes Peninsula since 1966 [e.g., Tryggvason, 1968, 1970, 1974, 1982; Eysteins-son, 1993], and repeated distance measurements were performed on the SW tip of the Reykjanes Peninsula from 1969 to 1979 [Calvert, 1969; Brander, 1973; Brander et al., 1976; Wood, 1982]. These measurements have indicated left-lateral movements parallel to the Reykjanes Peninsula seismic zone, extensional movements perpendicular to the seismic zone and subsidence of existing grabens. In addition, a local subsidence has been measured in the Svartsengi geothermal area, Reykjanes volcanic system (Figure 2), which is considered a result of geothermal exploitation in the area [Eysteins-son, 1993].

In 1986 the first GPS measurements were performed on the Reykjanes Peninsula when a countrywide GPS campaign was conducted in Iceland [Foulger et al., 1987, 1993]. Seven of the original nine GPS points located on the peninsula were remeasured in 1989 and 1992. The measurements from 1986 to 1992 indicate left-lateral strain accumulation on the peninsula [Sturkell et al., 1994; Sigmundsson et al., 1995]. The direction of max-

imum left-lateral shear strain estimated in the period 1986-1992 was  $N76^\circ \pm 6^\circ E$  with tensor shear strain rate of  $-0.222 \pm 0.0054 \mu\text{strain/yr}$  [Sturkell et al., 1994].

Vadon and Sigmundsson [1997] used satellite-based synthetic aperture radar (SAR) interferometry to measure crustal deformation from 1992 to 1995 on the Reykjanes Peninsula. The largest signal in their data was subsidence in the Svartsengi geothermal area at the rate of up to 13 mm/yr from 1992 to 1995. A weaker signal resulting from strain accumulation due to plate movements could also be detected, indicating left-lateral strain accumulation across the seismic zone and subsidence of the plate boundary at the rate of  $\sim 6.5$  mm/yr.

In 1993 a GPS network of 38 points was measured on the Reykjanes Peninsula. In 1998 the whole network was remeasured for the first time. The main purpose of the network was to allow more detailed study of the style of deformation at the Reykjanes Peninsula than previously possible. Here we present the results from these measurements. We attempt to explain the observed displacement field by three superimposed sources of deformation: strike-slip movement along the oblique plate boundary, magmatic inflation of the Hengill-Hrómundartindur volcanic system near

the eastern end of the peninsula, and subsidence due to man-made pressure reduction in the Svartsengi geothermal area in the western part of the peninsula.

## 2. Measurements and Analysis

### 2.1. GPS Measurements

In the 1993 GPS campaign, three dual-frequency Trimble 4000SST receivers were used. One of the receivers was operated continuously at a reference point in Reykjavík, ARNA, while other points in the network were measured. In the 1998 GPS campaign an International GPS Service (IGS) permanent tracking station in Reykjavík was used as a reference station. It has a dual-frequency Rogue SNR-8000 receiver. Three dual-frequency Trimble 4000SST receivers were used for the measurements of other points in the network. The former reference station, ARNA, was measured for 7 days during the 1998 measurements to enable accurate estimation of the position of REYK relative to ARNA. The

displacements from 1993 to 1998 were calculated relative to the ARNA station [Hreinsdóttir *et al.*, 1999].

All the measurements were divided into eight hour long sessions, and each point was measured for at least one whole session and part of two sessions. The Trimble 4000SST receivers collected data at 15 s intervals, while the IGS tracking station in Reykjavík collected data at 30 s intervals [Hreinsdóttir *et al.*, 1999].

### 2.2. Data Analysis

The data were analyzed with the Bernese GPS Software, version 4.0, [Rothacher and Mervart, 1996] using orbit information from the Center for Orbit Determination in Europe (CODE). No meteorological data were collected during the measurements. The Saastamoinen tropospheric refraction model was used to estimate site troposphere values.

In processing the 1993 data, precise orbit information from CODE, given in the ITRF91 reference frame [Boucher and Altamimi, 1996], were used to calcu-

Table 1. Site Deformation Rates Relative to Reykjavík<sup>a</sup>

Station	Latitude, °N	Longitude, °E	<i>H</i> , m	<i>v</i> <sub>north</sub> , mm/yr	<i>v</i> <sub>east</sub> , mm/yr	<i>v</i> <sub>up</sub> , mm/yr
GARD	64.0681	-22.6859	78.9	-1.8 ± 0.5	1.7 ± 0.5	3.3 ± 2.1
KINN	63.8706	-22.6849	99.5	-4.5 ± 0.5	6.3 ± 0.5	-8.3 ± 2.6
HAFN	63.9272	-22.6780	81.7	-4.3 ± 0.7	3.7 ± 0.5	-2.4 ± 2.6
RNES	63.8252	-22.6530	90.4	0.6 ± 0.7	8.4 ± 0.5	-9.2 ± 2.6
TJAL	63.8515	-22.6263	83.5	-1.1 ± 0.7	7.8 ± 0.5	-7.1 ± 2.7
HLBV	64.0291	-22.5601	94.4	-2.7 ± 0.5	2.6 ± 0.5	-2.9 ± 1.8
URDA	63.9266	-22.5590	107.3	-3.6 ± 0.7	4.7 ± 0.7	-3.3 ± 2.7
STAD	63.8208	-22.5232	81.3	3.9 ± 0.7	9.1 ± 0.5	-8.2 ± 2.8
THOF	63.8938	-22.5223	228.2	-3.9 ± 0.7	8.1 ± 0.5	-4.7 ± 0.7
GRIM	63.9716	-22.4258	139.7	-3.1 ± 0.5	2.5 ± 0.5	-3.4 ± 2.4
ARSE	63.9145	-22.4246	99.3	-3.8 ± 0.5	4.5 ± 0.5	-9.2 ± 1.9
SVAR	63.8792	-22.4232	88.5	0.8 ± 0.7	6.0 ± 0.5	-11.2 ± 2.5
VOGA	63.9737	-22.3434	99.6	-3.3 ± 0.7	2.6 ± 0.5	-8.2 ± 2.7
KAST	63.8800	-22.3232	143.6	0.7 ± 0.7	6.2 ± 0.5	-9.1 ± 2.7
NAUT	63.9184	-22.2881	191.8	-0.9 ± 0.7	4.0 ± 0.5	0.0 ± 2.7
KUAG	64.0022	-22.2349	126.1	-2.7 ± 0.7	1.8 ± 0.5	-2.8 ± 2.7
SELA	63.8459	-22.2344	80.7	0.4 ± 0.5	10.9 ± 0.5	-5.0 ± 1.9
SELS	63.9007	-22.1505	256.6	0.7 ± 0.8	7.7 ± 0.5	-3.6 ± 3.3
HOSK	63.9548	-22.1132	176.9	-2.0 ± 0.5	4.3 ± 0.5	-3.8 ± 2.6
KRIS	63.8674	-22.0895	196.2	-1.7 ± 0.7	1.0 ± 0.5	-0.9 ± 2.7
GRAE	64.0309	-22.1091	96.7	2.1 ± 0.7	10.0 ± 0.5	-3.0 ± 2.5
MOHA	63.9199	-22.0595	264.5	-0.9 ± 0.7	5.3 ± 0.5	-6.4 ± 2.2
LAMB	63.9103	-22.0126	206.8	-0.1 ± 0.7	6.4 ± 0.5	-4.1 ± 2.7
KLOF	63.9639	-21.9661	220.3	-1.1 ± 0.7	3.6 ± 0.5	-4.3 ± 2.6
ASFJ	64.0513	-21.9430	192.2	-0.8 ± 0.7	1.3 ± 0.5	-2.3 ± 2.3
BURF	64.0454	-21.8558	163.2	-0.3 ± 0.5	0.6 ± 0.5	2.7 ± 2.0
HERD	63.8691	-21.8391	79.1	-0.3 ± 0.5	10.7 ± 0.5	-1.0 ± 2.5
GRIN	63.9925	-21.7771	293.7	-1.6 ± 0.7	2.8 ± 0.5	1.9 ± 2.7
BREN	63.9457	-21.7671	525.6	0.3 ± 1.1	5.8 ± 1.1	2.5 ± 1.9
ULFA	64.1470	-21.7102	361.7	2.7 ± 0.8	-0.1 ± 0.8	4.4 ± 4.2
HOLM	64.0888	-21.7017	158.9	2.2 ± 0.5	0.2 ± 0.5	1.9 ± 2.4
STRA	63.8448	-21.6577	99.2	-1.5 ± 0.7	12.4 ± 0.5	3.1 ± 1.9
BLAF	63.9883	-21.6508	514.0	-0.9 ± 0.5	0.5 ± 0.5	-2.8 ± 2.1
HNUK	63.8752	-21.5701	253.8	-2.1 ± 0.6	12.3 ± 0.5	2.0 ± 2.1
KAFF	64.0611	-21.4847	309.2	2.0 ± 0.5	-3.1 ± 0.5	5.2 ± 2.4
THRE	63.9884	-21.4645	337.6	-1.7 ± 0.5	0.3 ± 0.5	6.5 ± 1.8
THOR	63.9086	-21.3654	106.9	-7.0 ± 0.7	11.3 ± 0.5	3.4 ± 2.5

<sup>a</sup>Reykjavík (ARNA) 64.14°N, -21.95°E, 91.7 m. *H*, Height; *v*, velocity.

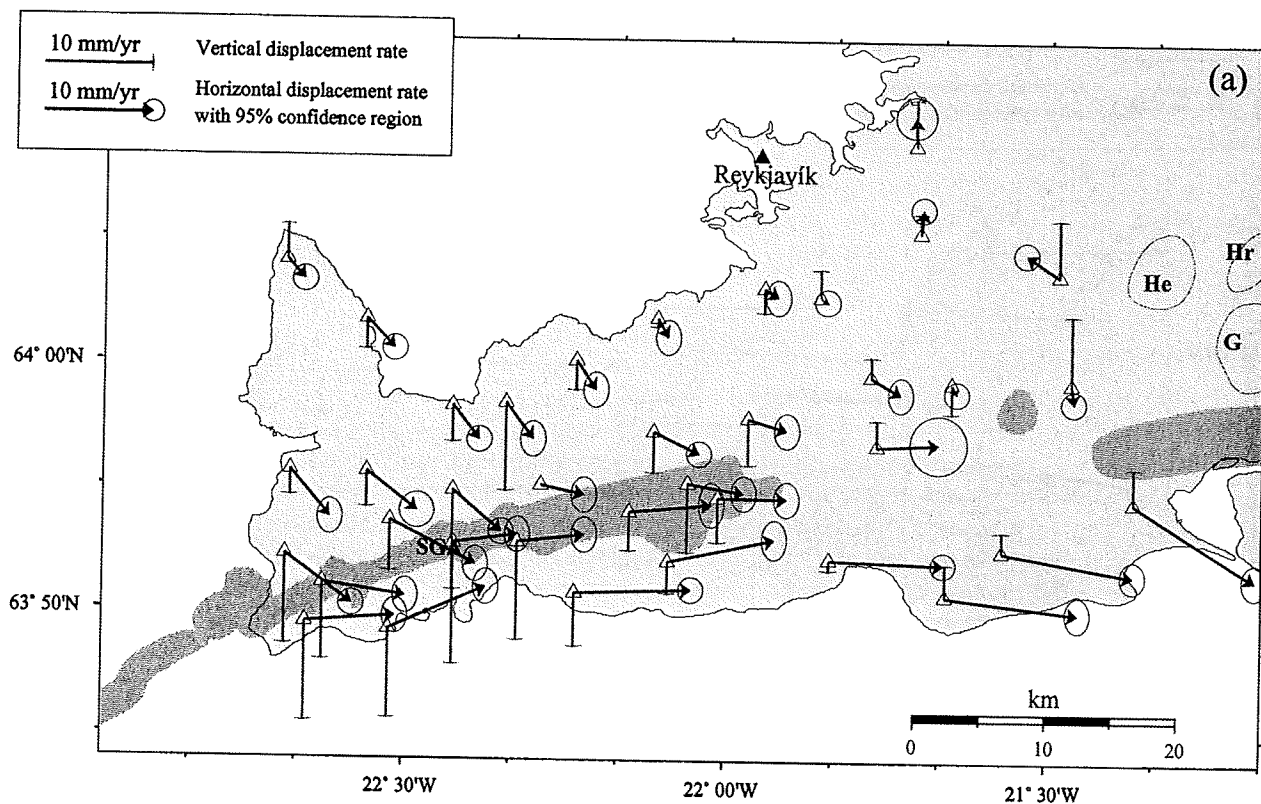


**Figure 3a.** Measured displacement rate in the period 1993-1998 relative to the reference station in Reykjavík. The errors in the vertical displacements are  $\sim 2$  mm/yr. SGA, Svartsengi geothermal area; He, Hengill volcanic system; Hr, Hrómundartindur volcanic system; G, Grensdalur volcanic system.

late point coordinates relative to the reference station. Data from the 1998 Reykjanes Peninsula GPS campaign were calculated relative to the IGS tracking station in Reykjavík using precise orbit information, given in the ITRF96 reference frame [Rothacher *et al.*, 1998].

Initially, each session was processed separately. Then the solutions for all the sessions were combined into a network solution [Hreinsdóttir *et al.*, 1999]. When processing each session, the estimation program gives formal errors which indicate the phase scatter. Systematic errors or mismodeled parameters are not taken into account, and the formal error can be unrealistic. For more realistic error estimation the scatter in the whole network solution was used to estimate a scaling factor for the formal uncertainties. We used Dynamic Adjustment Program (DYNAP) from the National Geodetic Survey to estimate the scaling factor and calculate the scaled formal errors for each set of point coordinates. The error estimation does not take into account potential errors in antenna position. To minimize this error, the position of each antenna was measured accurately before and after the measurements.

### 3. Crustal Deformation

The measured displacement rates relative to the reference station in Reykjavík are listed in Table 1. In Fig-

ure 3a the displacements are shown, horizontal displacement with solid vectors and vertical displacement with shaded bars. Using orbit determination in the ITRF reference frame, ITRF91 for the 1993 GPS campaign and ITRF96 for the 1998 GPS campaign, we hope to minimize possible reference frame errors. According to Boucher and Altamimi [1996], no rotation is expected between the reference frames, and given the size of the Reykjanes Peninsula GPS network (80 km  $\times$  40 km), small rotation should not have significant effect on the observed deformation.

The plate motion model NUVEL-1A predicts a velocity of  $18.8 \pm 0.5$  mm/yr in direction  $N77.2^\circ \pm 1.1^\circ W$  for Reykjavík relative to the Eurasian plate [DeMets *et al.*, 1990, 1994]. The IGS tracking station in Reykjavík was included in the global velocity field model GPSVEL 0.0 that is based on 4 years of data span [Blewitt *et al.*, 2000]. According to Blewitt *et al.* [2000], the velocity at Reykjavík is very similar to that predicted by the NUVEL-1A plate motion model, with  $\sim 2.5$  mm/yr less northward motion. Their velocity errors are at the level of 1 mm/yr (G. Blewitt personal communications, 2000). Using the result of Blewitt *et al.* [2000], a velocity vector of 18.5 mm/yr in direction  $N84.7^\circ W$  was assumed for the reference station. Other velocity vectors were adjusted accordingly (Figure 3b). To study the deformation on the Reykjanes Peninsula relative to

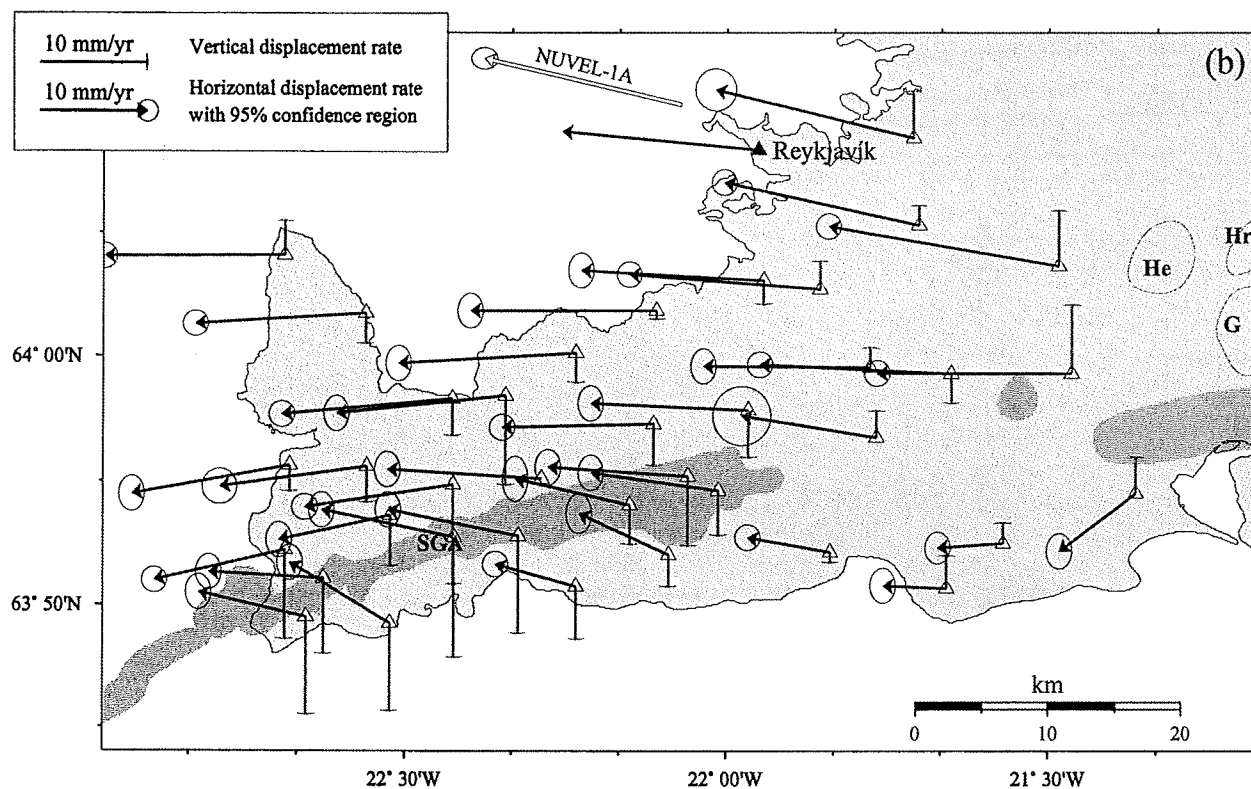


**Figure 3b.** Measured displacement rate in the period 1993-1998. The displacement of each GPS point is shown assuming that the velocity of the reference station in Reykjavik, relative to the Eurasian plate, is 18.5 mm/yr in direction N84.7°W. The NUVEL-1A predicted motion is shown for comparison. SGA, Svartsengi geothermal area; He, Hengill volcanic system; Hr, Hrómundartindur volcanic system; G, Grensdalur volcanic system.

the plate boundary rather than a fixed plate, we then subtracted half the expected NUVEL-1A velocity vector from all the sites (Figure 3c).

The observed displacements on the Reykjanes Peninsula from 1993 to 1998 show a pattern which can be interpreted in terms of strain accumulation in a left-lateral shear zone at depth striking about N76°E. The horizontal displacement vectors tend to be parallel to the seismic zone, given the assumed motion of Reykjavik. North of the zone the GPS points move toward the west, and south of the zone the GPS points move toward the east. The vertical displacement vectors show increased subsidence (relative to the reference station) toward the zone. The horizontal vectors, in general, increase in length with distance from the seismic zone, and at the same time, they tend to rotate away from the zone.

There are some departures from the general picture described above. In the easternmost part of the Reykjanes Peninsula, the Hengill area, we observe expansion. Instead of subsidence toward the seismic zone, as observed in the western part of the peninsula, the points are rising. The horizontal displacements are also larger than observed in other parts of the peninsula. Two active volcanic systems, Hengill and Hrómundartindur, and the extinct Grensdalur volcanic system are located

in the Hengill area. *Sigmundsson et al.* [1997] concluded from geodetic and seismic measurements that surface deformation and increased seismicity was caused by magma accumulation in the roots of the Hrómundartindur volcanic system in the 1991-1995 period. GPS measurements conducted in the Hengill area in 1995 and 1998 indicate continued inflation in the Hengill area [*Hreinsdóttir*, 1999]. This episode of magma accumulation appears to have begun in 1993 and ended in 1998. The inflation has also been observed with interferometric SAR (InSAR) measurements [*Feigl et al.*, 2000]. Here inflation is detected on points in the easternmost part of the Reykjanes Peninsula GPS network, 15-25 km southwest of the inflation center.

Another signal, quite the opposite to the one in the Hengill area, is observed in the western part of the peninsula, in the area of the Svartsengi geothermal area (SGA). The area is contracting, most likely in response to exploitation of the geothermal field by the Svartsengi power station. The maximum subsidence measured on the peninsula,  $60 \pm 10$  mm in 5 years, occurred in this area, at a point next to the Svartsengi power station. *Eysteinnsson* [1993] observed subsidence in this area using leveling from 1975 to 1992, and *Vadon and Sigmundsson* [1997] also documented subsidence with satellite-based SAR interferometry from 1992 to 1995.

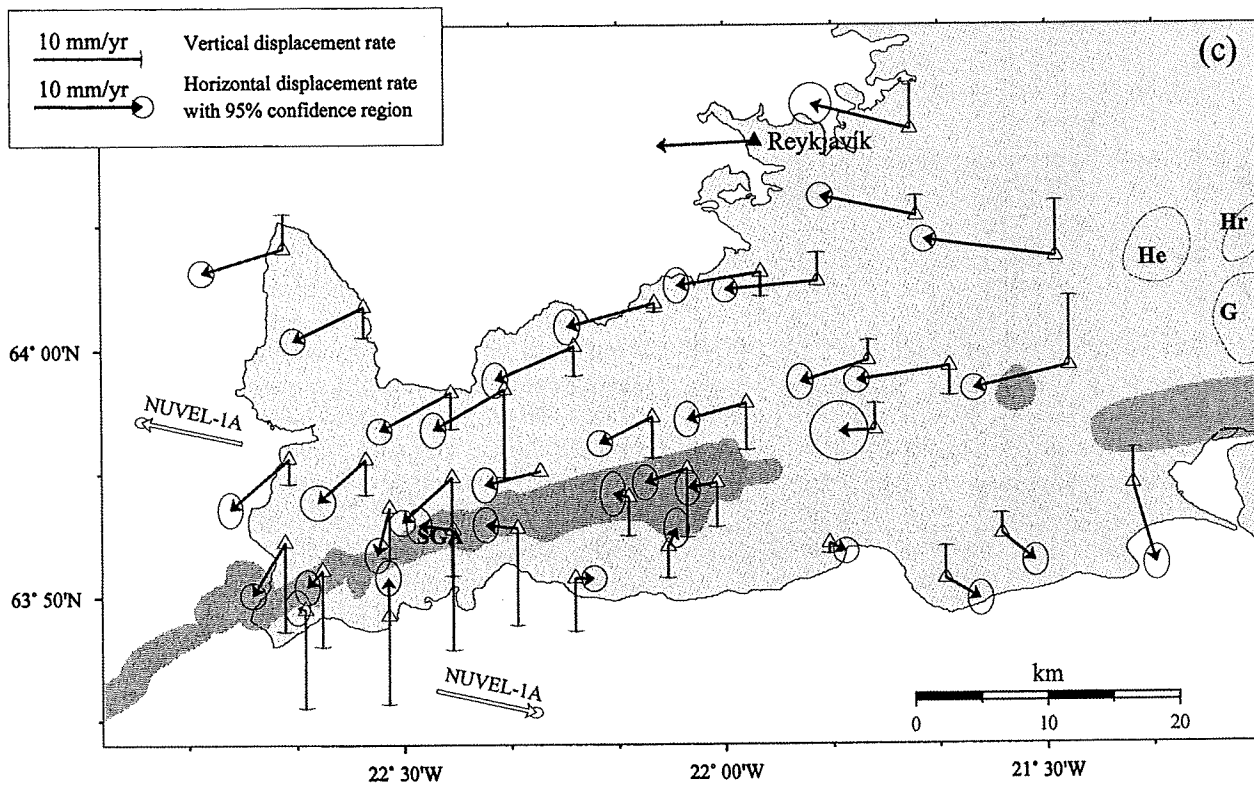


**Figure 3c.** Measured displacement rate in the period 1993-1998. Half the NUVEL-1A predicted motion (Figure 3b) has been subtracted from each velocity vector to study the deformation relative to the plate boundary rather than fixed plate. The NUVEL-1A predicted motion is shown for comparison. SGA, Svartsengi geothermal area; He, Hengill volcanic system; Hr, Hrómundartindur volcanic system; G, Grensdalur volcanic system.

The average rate of subsidence measured from 1993 to 1998 with GPS,  $\sim 12$  mm/yr, is similar to the average rate determined from the leveling measurements from 1975 to 1982 ( $\sim 14$  mm/yr) [Eysteinnsson, 1993] and the InSAR measurements from 1992 to 1995 ( $\sim 13$  mm/yr) [Vadon and Sigmundsson, 1997]. Measurements made at other time periods and shorter time intervals suggest that the subsidence rate varies from one year to another [Eysteinnsson, 1993; Vadon and Sigmundsson, 1997].

Observed displacements near the central axis of the plate boundary, in the Reykjanes Peninsula seismic zone, are more irregular than elsewhere on the peninsula. Some of the points move orthogonally to the seismic zone rather than parallel to it and their velocity is larger than should be expected. The observed deformation in the zone could be a result of displacement of blocks within the seismic zone. The density of the network and the accuracy of the measured displacement vectors is not sufficient to verify this directly.

#### 4. Plate Boundary

The observed displacements resemble those expected at a transform zone and observed at the SISZ [Sigmundsson et al., 1995]. The measurements from 1993 to

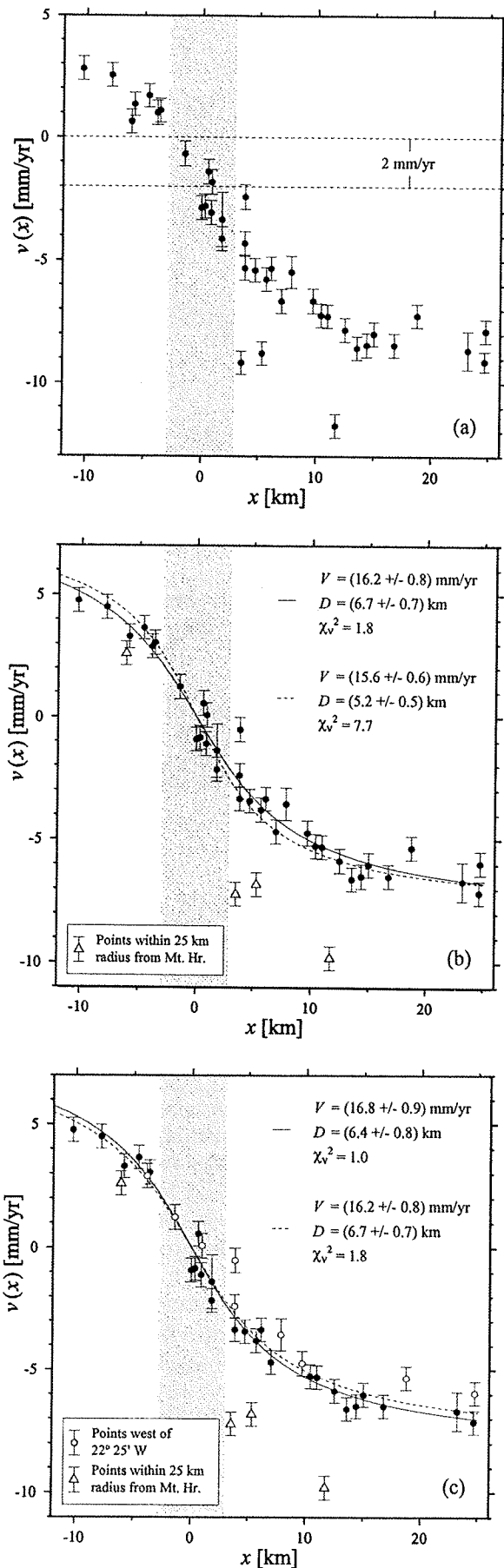
1998 show that left-lateral strain is accumulating across the peninsula at a rate of about

$$\begin{aligned} \dot{\epsilon}_{yx} &= \frac{1}{2} \frac{\partial \dot{w}_y}{\partial x} \\ &\approx \frac{1}{2} \frac{(-13 \text{ mm/yr})}{35 \text{ km}} = -0.2 \mu\text{strain/yr}, \quad (1) \end{aligned}$$

where  $x$  is the maximum distance between GPS points perpendicular to the plate boundary and  $w_y$  is their relative displacement rate parallel to the plate boundary. This is consistent with GPS measurements from 1986 to 1992 that show tensor shear strain rate of  $-0.222 \pm 0.0054 \mu\text{strain/yr}$  in direction  $N76^\circ \pm 6^\circ E$  [Sturkell et al., 1994].

We determine how well the measurements fit a simple transcurent motion model in a uniform elastic half-space. We use a simple screw dislocation model assuming that the uppermost part of the crust does not slip and is locked down to a certain depth, the locking depth of the brittle crust. Below it the plates slide past each other at a constant rate. The interseismic displacement at the surface is then related to the perpendicular distance to the plate boundary  $x$ , the uniform slip rate beneath the locking depth  $V$ , and the locking depth of the crust  $D$  [Savage and Burford, 1973]:





$$v(x) = V\pi^{-1} \arctan(x/D). \quad (2)$$

Fault ruptures found in or near the Reykjanes Peninsula seismic zone and seismic studies indicate that the left-lateral deformation observed along the seismic zone is accomplished by right-lateral motion on many parallel N-S trending strike slip faults (bookshelf-style deformation) (P. Einarsson et al., manuscript in preparation, 2001). For simplification, we assume that the transcurrent motion is a result of strain accumulation on a left-lateral shear zone along the seismic zone. The seismic zone bends in the westernmost part of the peninsula. To resemble that, we allow the shear zone to bend at  $22^\circ 25' W$ . The shear zone parameters that best fit the measurements give a shear zone that strikes  $N79^\circ E$  east of  $22^\circ 25' W$  but  $N72^\circ E$  west of  $22^\circ 25' W$ . The shear zone's strike and location fit reasonably well with seismic studies and the location of faults ruptures in the seismic zone.

We use each point's velocity parallel to the shear zone and distance perpendicular to the shear zone as data and estimate the best fitting values for the deep slip rate and the locking depth using weighted least squares inversion [Menke, 1984]. The interseismic displacement is a nonlinear function of the locking depth  $D$  (equation (2)). We linearize the equation using Taylor Series about a nominal  $D = D^{est}$  and estimate the difference  $\Delta D = D - D^{est}$  in the inversion. Using reasonable starting values for the locking depth and deep slip rate, we iterate the inversion until the solution converges.

Figure 4a shows the velocity parallel to the Reykjanes Peninsula seismic zone as a function of the distance perpendicular to the seismic zone. The velocity field does not reveal symmetry over the seismic zone given the assumed velocity of Reykjavik ( $9.2$  mm/yr in direction  $N92.5^\circ W$ ). Instead, the velocity field seems to be offset by a few mm/yr. It is possible that the deformation across the Reykjanes Peninsula seismic zone is nonsymmetric. The reason for the observed nonsymmetry could also be due to the assumed velocity of the reference station, Reykjavik. Uncertainties in the NUVEL-1A plate motion model ( $0.5$  mm/yr) and uncertainties in the results of Blewitt et al. [2000] ( $\sim 1$  mm/yr) have not been taken into account. In addition, it is possible that the

**Figure 4.** Velocity parallel to the seismic zone versus perpendicular distance to the seismic zone. (a) A velocity correction term of  $2$  mm/yr, which had to be added to the data to get symmetry over the seismic zone. (b) The best fitting screw dislocation model for all the peninsula (dashed line), excluding four points next to the inflating mount Hrómundartindur (solid line). (c) Best fitting screw dislocation model excluding four points next to the inflating mount Hrómundartindur (dashed line) and nine points in the westernmost part of the peninsula (solid line).



NUVEL-1A plate motion model is slightly biased for the North American-Eurasian plate pair. To correct for this nonsymmetry problem, we repeated the inversion several times, adding extra velocity to all the data to find a correction term that best fits the inversion. Owing to the general strike of the plate boundary the inversion is not very sensitive to a change in the northward motion. We therefore kept the north component of the velocity fixed but changed the east component to find a best fit. As a result we added a velocity vector of 2.0 mm/yr in direction N90°E to all the points. It is noteworthy that any change in the northward motion does change this result slightly; for every  $\delta v_{\text{north}} = \pm 0.1$  mm/yr we get an extra  $\delta v_{\text{east}} = \mp 0.02$  mm/yr.

The results of the inversion, using the estimated velocity correction term, are shown in Figures 4b and 4c. When including all the points, the inversion gives a deep slip rate of  $V = (15.6 \pm 0.6)$  mm/yr and a locking depth of  $D = (5.2 \pm 0.5)$  km. The  $\chi^2_{\nu}$  for this model is 7.7. The majority of the data fit the screw dislocation model within their uncertainties (Figure 4b). Some of the points, however, show displacements that are significantly different from the model estimations. This suggests that signals other than uniform left-lateral strain accumulation across the seismic zone affect the data.

Geodetic measurements in the Hengill area indicate magma accumulation beneath the Hrómundartindur volcanic system in the period [e.g., *Sigmundsson et al.*, 1997]. In addition, a  $m_b$  5.1 earthquake occurred west of mount Hrómundartindur in June 1998, a month before the second GPS campaign was performed [*Thorbergsson and Vigfússon*, 1998; *Ágústsson*, 1998; *Árnadóttir et al.*, 1999]. Excluding four points next to Hrómundartindur volcano, we get a significantly better fit to the data.

The inversion gives a deep slip rate of  $V = (16.2 \pm 0.8)$  mm/yr and a locking depth of  $D = (6.7 \pm 0.7)$  km with  $\chi^2_{\nu} = 1.8$  (Figure 4b).

Points in the westernmost part of the peninsula also show significantly different motion from the estimated best fitting model. We therefore excluded points west of 22°25'W as well as four points next to Hrómundartindur volcano (Figure 4c). We obtain a good fit to the points in the eastern part of the peninsula (solid line) with a deep slip rate of  $V = (16.8 \pm 0.9)$  mm/yr and a locking depth of  $D = (6.4 \pm 0.8)$  km, giving  $\chi^2_{\nu} = 1.0$ . The difference between the two models, with and without the westernmost part of the peninsula (Figure 4c), is not significant.

The locking depth and deep slip rate are highly correlated. In Figure 5 the trade-off between model parameters for these two inversions are shown. A locking depth of 6.5 km is in a good agreement with seismic observations which have indicated that majority of earthquakes on the peninsula occur at depths of  $\sim 1$ -5 km [*Klein et al.*, 1973, 1977; *A. Tryggvason et al.*, submitted manuscript, 2000]. The estimated deep slip rate of  $16.8 \pm 0.9$  mm/yr is also consistent with the NUVEL-1A plate motion parallel to the seismic zone ( $16.8 \pm 0.6$  mm/yr in direction N76°  $\pm$  3°E).

The comparison of the measurements to the best fitting model are shown in Figure 6. To reveal the remaining signal(s), we use the model estimated excluding both points next to Hrómundartindur volcano and points in the westernmost part of the peninsula, locking depth of 6.4 km, and deep slip rate of 16.8 mm/yr. The fit to the observations is reasonable, but there are obvious misfits in the easternmost part of the peninsula, increasing toward the Hengill area, and the model fails to

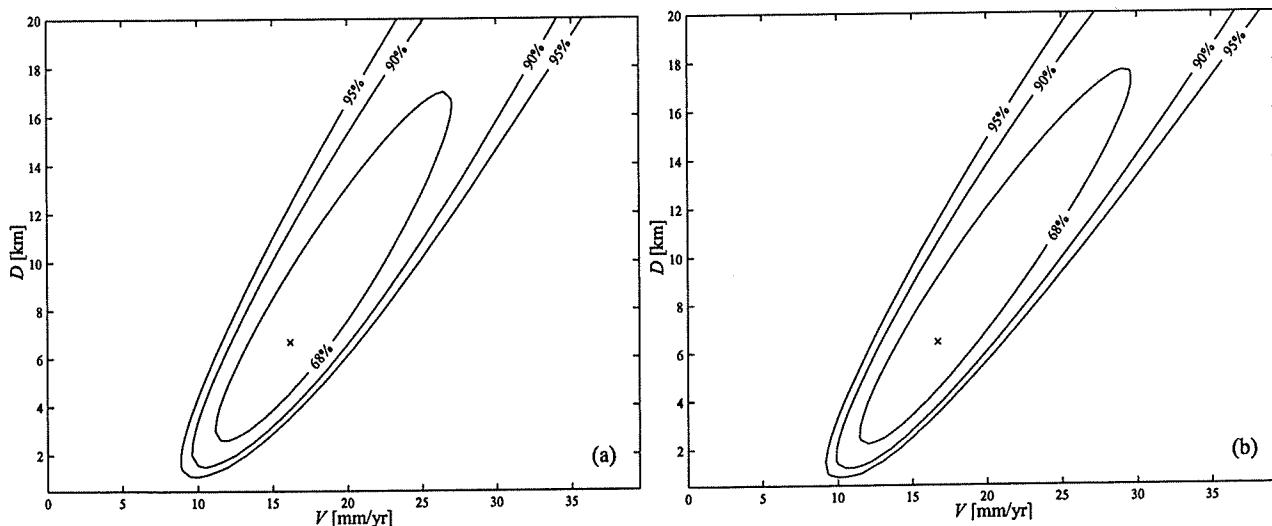


**Figure 5.** Contour plots of  $\chi^2$  showing the trade-off between model parameters, the deep slip rate, and the locking depth. The cross shows the best fitting model. (a) The best fitting screw dislocation model for all the peninsula, excluding points next to the inflating mount Hrómundartindur. (b) The best fitting screw dislocation model excluding four points next to the inflating mount Hrómundartindur and nine points in the westernmost part of the peninsula.